

# Accurate Performance Analysis of Hadamard Ratio Test for Robust Spectrum Sensing

Lei Huang, *Member, IEEE*, Yuhang Xiao, Hing Cheung So, *Senior Member, IEEE*, and Jun Fang, *Member, IEEE*

**Abstract**—Hadamard ratio test is a well-known approach to robust signal detection in multivariate analysis. Recently, it has been exploited for robust spectrum sensing in cognitive radio, but its detection performance is not yet completely analyzed. This work is devoted to accurate detection performance analysis of the Hadamard ratio method for robust spectrum sensing. By computing the first and second exact negative moments for the signal-presence hypothesis along with employing the Beta distribution approximation, we derive accurate analytic formulae for detection probability. This enables us to theoretically evaluate the detection behavior of the Hadamard ratio test. Numerical results are presented to validate our theoretical findings.

**Index Terms**—Cognitive radio, spectrum sensing, generalized likelihood ratio test, Beta distribution, multiple antennas, robustness.

## I. INTRODUCTION

TO alleviate spectrum deficiency resulting from the policies of fixed spectrum allocation [1], cognitive radio (CR) [2]–[8] has been put forward as a potential paradigm for future communications. In a CR network, a secondary (unlicensed) user (SU) is allowed to borrow the frequency channels from the primary (licensed) users (PUs) provided that it does not cause intolerable interference to the latter. In order to maximize spectral utilization and minimize harmful interference to the PUs, the SU usually needs to employ multiple antennas to reliably detect the PUs particularly at low signal-to-noise ratio (SNR) and/or small sample size. However, the multi-antenna receiver is typically uncalibrated or contains calibration error in practice. Under such environments, the energy detection (ED) approach [9]–[11] and eigenvalue-based detectors [12]–[19] cannot provide reliable sensing performance. This is because all of them

are devised from the assumption of independent and identically distributed (IID) observations. This thereby calls for the development of robust methodology for practical spectrum sensing.

To handle non-IID noise, numerous robust detection approaches have been put forward for spectrum sensing, such as the Hadamard ratio test [20]–[22], Gerschgorin disk test [23], locally most powerful invariant test (LMPIT) [24], [25] and volume-based test [26]. As the Hadamard ratio detector is robust against the non-IID noise and originally derived in the framework of generalized likelihood ratio test (GLRT), it has received much attention [27]–[30]. In this approach, signal detection is formulated as the issue of distinguishing between a diagonal matrix and an arbitrary Hermitian matrix. A variant of the Hadamard ratio approach for spectrum sensing has been proposed in [27], in which the number of PUs needs to be known *a priori* to the receiver. On the other hand, the performance of the Hadamard ratio algorithm for spectrum sensing has been studied in [29], [30]. Nevertheless, only the false-alarm probability is analyzed in [30]. Although both false-alarm and detection probabilities have been calculated in [29], the accuracy of the detection probability is not yet accurate enough. In particular, the asymptotic non-central Chi-square approximation in [29] ignores the term  $\mathcal{O}(1/N)$  with  $N$  being the number of samples, which is valid only when  $N$  is large enough but not appropriate when  $N$  is small. As a matter of fact,  $N$  is usually small and comparable with the number of antennas in multi-antenna CR receiver [12], [17], [31]. Under such conditions, the approximate formulae in [29] cannot offer accurate prediction for the detection performance of the Hadamard ratio test.

In this paper, the theoretical detection probability of the Hadamard ratio test is derived, which turns out to be more accurate than the calculation in [29]. In particular, we compute the first and second exact negative moments<sup>1</sup> of the Hadamard ratio statistic under the signal-presence hypothesis. With the so-obtained moments, we derive accurate closed-form approximation for the test statistic distribution under the signal-presence hypothesis by matching its moments to those of the Beta distribution. In the sequel, the detection probability is produced in terms of the analytic formulae.

The remainder of the paper is organized as follows. In Section II, we present the signal model, formulate the sensing problem and review the solution based on the Hadamard ratio test. Performance analysis of the Hadamard ratio method is provided in Section III. Simulation results are presented in Section IV. Finally, conclusions are drawn in Section V.

<sup>1</sup>For more details about the negative moments, the interested reader is referred to [32]–[34].

Manuscript received April 15, 2014; revised July 29, 2014; accepted September 15, 2014. Date of publication September 19, 2014; date of current version February 6, 2015. This work was supported in part by a grant from the NSFC/RGC Joint Research Scheme sponsored by the Research Grants Council of Hong Kong and the National Natural Science Foundation of China (Project No.: N\_CityU 104/11, 61110229/61161160564), by the National Natural Science Foundation of China under Grants 61222106 and 61171187, and by the Shenzhen Kongqie talent program under Grant KQC201109020061A. The associate editor coordinating the review of this paper and approving it for publication was S. Jin.

L. Huang and Y. Xiao are with the Department of Electronic and Information Engineering, Harbin Institute of Technology Shenzhen Graduate School, Shenzhen 518005, China (e-mail: dr.lei.huang@ieee.org; yuhangxiao@outlook.com).

H. C. So is with the Department of Electronic Engineering, City University of Hong Kong, Kowloon, Hong Kong (e-mail: hcs@ee.cityu.edu.hk).

J. Fang is with the National Key Laboratory of Science and Technology on Communications, University of Electronic Science and Technology of China, Chengdu 611731, China (e-mail: JunFang@uestc.edu.cn).

Color versions of one or more of the figures in this paper are available online at <http://ieeexplore.ieee.org>.

Digital Object Identifier 10.1109/TWC.2014.2359223

Throughout this paper, we use boldface uppercase letter for matrix, boldface lowercase letter for column vector or collection, and lowercase letter for scalar. Superscripts  $(\cdot)^T$  and  $(\cdot)^H$  represent transpose and conjugate transpose, respectively. The  $\mathbb{E}\{a\}$  and  $\hat{a}$  denote the expected and estimated values of  $a$ , respectively. The  $\text{tr}(\mathbf{A})$  and  $|\mathbf{A}|$  are the trace and determinant of  $\mathbf{A}$ , respectively. The  $\text{diag}(\mathbf{A})$  stands for a diagonal matrix composed of the diagonal elements of  $\mathbf{A}$ . The  $\mathbf{I}_M$  is the  $M \times M$  identity matrix. The  $\mathbf{x} \sim \mathcal{N}(\boldsymbol{\mu}, \boldsymbol{\Sigma})$  means that  $\mathbf{x}$  is complex Gaussian distributed with mean  $\boldsymbol{\mu}$  and covariance matrix  $\boldsymbol{\Sigma}$ , and  $\sim$  signifies “distributed as”. The  $\mathcal{W}_M(N, \boldsymbol{\Sigma})$  stands for the complex Wishart distribution with  $N$  degrees of freedom (DOFs).

## II. PROBLEM FORMULATION

### A. Signal Model

Consider a multiple-input multiple-output (MIMO) CR network where the SU has  $M$  antennas to receive the signals emitted by  $d$  PUs with a single antenna. The output of the SU,  $\mathbf{x}_n (n = 1, \dots, N)$ , under the binary hypotheses, can be written as

$$\mathbf{x}_n = \begin{cases} \mathbf{v}_n, & \mathcal{H}_0 \\ \mathbf{H}\mathbf{s}_n + \mathbf{v}_n, & \mathcal{H}_1 \end{cases} \quad (1)$$

where  $\mathcal{H}_0$  denotes the signal-absence hypothesis while  $\mathcal{H}_1$  denotes the signal-presence hypothesis. Here,  $\mathbf{H} \in \mathbb{C}^{M \times d}$  denotes the MIMO channel coefficient matrix between the PUs and SU, which is unknown deterministic during the sensing period. The

$$\mathbf{x}_n = [x_1(n), \dots, x_M(n)]^T \quad (2)$$

$$\mathbf{s}_n = [s_1(n), \dots, s_d(n)]^T \quad (3)$$

$$\mathbf{v}_n = [v_1(n), \dots, v_M(n)]^T \quad (4)$$

stand for the observation, signal and noise vectors, respectively. We assume that  $s_i(n) \sim \mathcal{N}(0, \sigma_{s_i})$  ( $i = 1, \dots, d$ ) with  $\sigma_{s_i}$  being the  $i$ th unknown signal variance, and  $v_i(n) \sim \mathcal{N}(0, \sigma_{v_i})$  ( $i = 1, \dots, M$ ) with  $\sigma_{v_i}$  being the unknown noise variance. Note that  $\sigma_{v_i}$  is not necessarily equal to  $\sigma_{v_j}$  for  $i \neq j$  in practice, which corresponds to the case of uncalibrated receiver. It is also assumed that the noises are statistically independent of each other and also independent of the signals. The problem at hand is to decide whether the primary signals exist or not from the noisy observations  $\mathbf{X} = [\mathbf{x}_1, \dots, \mathbf{x}_N]$ .

### B. Sensing Solution

For the binary hypotheses, the observation vector is assumed to be Gaussian distributed, i.e.,

$$\mathbf{x}_n | \mathcal{H}_i \sim \mathcal{N}(\mathbf{0}, \boldsymbol{\Sigma}^{(i)}), \quad i = 0, 1. \quad (5)$$

With the assumptions above, the covariance matrix under  $\mathcal{H}_0$  is given as  $\boldsymbol{\Sigma}^{(0)} = \text{diag}(\sigma_{v_1}, \dots, \sigma_{v_M})$ , but, under  $\mathcal{H}_1$ , defined as  $\boldsymbol{\Sigma}^{(1)} \triangleq (\sigma_{ij})_{M \times M}$  with  $\sigma_{ij}$  being the  $(i, j)$  entry of  $\boldsymbol{\Sigma}^{(1)}$ , which is non-diagonal and positive definite. Accordingly, the likelihood function under hypothesis  $\mathcal{H}_i$  is

$$L(\mathbf{X} | \mathcal{H}_i) = |\boldsymbol{\Sigma}^{(i)}|^{-N} \exp\left(-N \text{tr}\left(\left[\boldsymbol{\Sigma}^{(i)}\right]^{-1} \mathbf{S}\right)\right) \quad (6)$$

where  $\mathbf{S} = (1/N) \sum_{n=1}^N \mathbf{x}_n \mathbf{x}_n^H$  is the sample covariance matrix (SCM). Note that the constant term in (6) has been dropped for simplicity. It is easy to obtain the negative log-likelihood function of  $\mathbf{X}$  as

$$\mathcal{L}(\mathbf{X} | \boldsymbol{\Sigma}^{(i)}) = N \log |\boldsymbol{\Sigma}^{(i)}| + N \text{tr}\left(\left[\boldsymbol{\Sigma}^{(i)}\right]^{-1} \mathbf{S}\right). \quad (7)$$

Setting the derivative of  $\mathcal{L}(\mathbf{X} | \boldsymbol{\Sigma}^{(i)})$  with respect to  $\boldsymbol{\Sigma}^{(i)}$  to zero, we obtain the maximum likelihood (ML) estimates of  $\boldsymbol{\Sigma}^{(0)}$  and  $\boldsymbol{\Sigma}^{(1)}$  as  $\hat{\boldsymbol{\Sigma}}^{(0)} = \text{diag}(\mathbf{S})$  and  $\hat{\boldsymbol{\Sigma}}^{(1)} = \mathbf{S}$ , respectively. Let  $\mathbf{R} = N\mathbf{S}$  and  $\mathbf{D} \triangleq \text{diag}(\mathbf{R}) = \text{diag}(r_{11}, \dots, r_{MM})$  with  $r_{ii}$  ( $i = 1, \dots, M$ ) being the diagonal element of  $\mathbf{R}$ . The GLRT test statistic is

$$\frac{L(\mathbf{X} | \mathcal{H}_1)}{L(\mathbf{X} | \mathcal{H}_0)} = \frac{|\mathbf{R}|^N}{|\mathbf{D}|^N}. \quad (8)$$

It is easy to observe that (8) is an increasing function of  $|\mathbf{R}|/|\mathbf{D}|$ . Recall that a monotonic transformation of a test statistic does not vary its outcome provided that the decision threshold is revised accordingly. In the sequel, the GLRT statistic can be expressed in the form of “Hadamard ratio”, that is,

$$\xi = \frac{|\mathbf{R}|}{|\mathbf{D}|}. \quad (9)$$

In other words, the Hadamard ratio test is exactly the GLRT for this situation. When the primary signals exist, the determinant of  $\mathbf{R}$  considerably decreases, providing a good indicator for spectrum sensing. Consequently, if  $\xi$  is smaller than a preassigned decision threshold  $\gamma$ , the detector declares  $\mathcal{H}_1$ , otherwise,  $\mathcal{H}_0$ , i.e.,

$$\xi \underset{\mathcal{H}_1}{\overset{\mathcal{H}_0}{\geq}} \gamma. \quad (10)$$

The Hadamard ratio test statistic in (9) has been derived in [20] in the context of multivariate statistical analysis, later on reformulated in array processing for Gaussian signal detection [21], [22] and recently employed for spectrum sensing [27], [29], [30]. Nevertheless, performance analysis for the Hadamard ratio detector has not yet been completely investigated particularly in the context of spectrum sensing. In the next section, accurate analytic formula is derived for the detection probability. This enables us to theoretically evaluate the detection performance of the Hadamard ratio approach.

## III. DETECTION PERFORMANCE ANALYSIS

Usually, it is very difficult to determine the explicit expression for the distribution of  $\xi$  at arbitrary antenna number  $M$ . Consequently, it is desired to approximate the distribution as some known distribution with the same support by means of fitting their first several moments. As a matter of fact,  $\xi$  has the same support as the Beta distribution. In particular, note that  $\mathbf{R}$  is non-negative definite, meaning that  $|\mathbf{R}| \geq 0$ . Moreover, notice that  $r_{ii} > 0$  ( $i = 1, \dots, M$ ). As a result, we have  $\xi \geq 0$ . On the other hand, invoking the Hadamard’s inequality [35, p. 477], that is,  $|\mathbf{R}| \leq |\mathbf{D}|$ , we obtain

$$\xi = \frac{|\mathbf{R}|}{|\mathbf{D}|} \leq 1. \quad (11)$$

Thus, the test statistic  $\xi$  has the support of  $[0,1]$  which is the same as the Beta distribution. This enables us to utilize the moment-matching Beta approximation to determine its cumulative distribution function (CDF). To this end, we first determine the moments of  $\xi$  and then establish the detection probability by matching the moments to the Beta distribution with the same support. Indeed, the moment-matching approximation has been widely adopted in the literature, such as [18], [19], [30], [36], [37], to determine the distribution of various tests.

The  $k$ -th moment of  $\xi$ , denoted by  $\mathcal{M}_k$ , is provided in the following proposition.

*Proposition 1:* For any antenna number  $M$  and sample number  $N$ , the  $k$ -th moment of  $\xi$  under  $\mathcal{H}_1$  is

$$\mathcal{M}_k \triangleq \mathbb{E}[\xi^k] = \frac{|\Sigma^{(1)}|^k \Gamma_M(N+k)}{\Gamma_M(N)} T_{-k}, \quad k = -1, -2 \quad (12)$$

where  $\Gamma(\cdot)$  denotes the complete Gamma function and

$$\Gamma_M(N) = \pi_0^{\frac{1}{2}M(M-1)} \Gamma(N) \Gamma(N-1) \cdots \Gamma(N-M+1) \quad (13)$$

with  $\pi_0$  being the circumference ratio. Moreover,  $T_1$  and  $T_2$  are calculated as

$$T_1 = \frac{1}{i^M} \sum_{\pi \in \mathcal{S}_M} \frac{\Gamma(N-1+p(\pi))}{\Gamma(N-1)} (-1)^{p(\pi)} \prod_{m=1}^{p(\pi)} \nu(\pi_m) \quad (14a)$$

$$T_2 = \frac{1}{i^{2M}} \sum_{\pi \in \mathcal{S}_{2M}} \frac{\Gamma(N-2+p(\pi))}{\Gamma(N-2)} (-1)^{p(\pi)} \prod_{m=1}^{p(\pi)} \nu(\pi_m) \quad (14b)$$

where  $i = \sqrt{-1}$ ,  $\mathcal{S}_M$  consists of all the partitions of the  $M$ -element set  $\{t_1, \dots, t_M\}$ ,  $\mathcal{S}_{2M}$  is composed of all the partitions of the  $2M$ -element set  $\{t_1, t_1^*, \dots, t_M, t_M^*\}$ . Moreover, in (14a),  $\pi$  denotes a partition of  $\{t_1, \dots, t_M\}$  which is defined as a family of nonempty, pairwise disjoint subsets of  $\{t_1, \dots, t_M\}$  whose union is  $\{t_1, \dots, t_M\}$ ,<sup>2</sup>  $p(\pi)$  is the number of subsets in  $\pi$ ,  $\pi_m$  is the  $m$ -th subset of  $\pi$  for  $m = 1, \dots, M$ ,

$$\nu(\pi_m) = \frac{\partial^j |\mathbf{A}|}{\partial \pi_{m1} \cdots \partial \pi_{mj}} \Big|_{\mathbf{D}_t=0} \quad (14c)$$

and

$$|\mathbf{A}| = \left| \mathbf{I}_M - i \mathbf{D}_t \Sigma^{(1)} \right| \quad (15)$$

with  $\mathbf{D}_t = \text{diag}(t_1, \dots, t_M)$ . Furthermore,  $j$  is the number of elements in  $\pi_m$  and  $\pi_{mj}$  is the  $j$ -th entry of  $\pi_m$ . The definitions above are also applied to (14b). Additionally,  $t_m^*$  ( $m = 1, \dots, M$ ) is equal to  $t_m$  ( $m = 1, \dots, M$ ) in value but different in index.

*Proof:* The proof is given in Appendix A.  $\blacksquare$

<sup>2</sup>For more details about the partition of a finite nonempty set, the interested reader is referred to [38].

Note that the calculation of  $\nu(\pi_m)$  in (14c) requires the following formulae:

$$\frac{\partial |\mathbf{A}|}{\partial t_1} \Big|_{\mathbf{D}_t=0} = \begin{vmatrix} -i\sigma_{11} & -i\sigma_{12} & \cdots & -i\sigma_{1M} \\ 0 & 1 & \cdots & 0 \\ \vdots & \vdots & \ddots & \vdots \\ 0 & 0 & \cdots & 1 \end{vmatrix} \quad (16)$$

$$\frac{\partial^2 |\mathbf{A}|}{\partial t_1 \partial t_2} \Big|_{\mathbf{D}_t=0} = \begin{vmatrix} -i\sigma_{11} & -i\sigma_{12} & -i\sigma_{13} & \cdots & -i\sigma_{1M} \\ -i\sigma_{21} & -i\sigma_{22} & -i\sigma_{23} & \cdots & -i\sigma_{2M} \\ 0 & 0 & 1 & \cdots & 0 \\ \vdots & \vdots & \vdots & \ddots & \vdots \\ 0 & 0 & 0 & \cdots & 1 \end{vmatrix} \quad (17)$$

$$\frac{\partial^M |\mathbf{A}|}{\partial t_1 \partial t_2 \cdots \partial t_M} \Big|_{\mathbf{D}_t=0} = (-i)^M |\Sigma^{(1)}|. \quad (18)$$

Moreover, the term  $\nu(\pi_m)$ , which includes both  $t_m$  and  $t_m^*$ , such as  $\frac{\partial^2 |\mathbf{A}|}{\partial t_m^2} = 0$  and  $\frac{\partial^3 |\mathbf{A}|}{\partial t_{m-1} \partial t_m^2} = 0$ , is equal to zero.

For the simplest case where  $M = 2$ , it follows from (15) that

$$|\mathbf{A}| = \begin{vmatrix} 1 - it_1 \sigma_{11} & -it_1 \sigma_{12} \\ -it_2 \sigma_{21} & 1 - it_2 \sigma_{22} \end{vmatrix} \quad (19)$$

which, when inserted into (14), leads to

$$T_1 = -(N-1)(\sigma_{11}\sigma_{22} - \sigma_{12}\sigma_{21}) + N(N-1)\sigma_{11}\sigma_{22} \quad (20a)$$

$$T_2 = (N-2)(N-1)N(N+1)\sigma_{11}^2\sigma_{22}^2 - 4(N-2)(N-1)N\sigma_{11}\sigma_{22}(\sigma_{11}\sigma_{22} - \sigma_{12}\sigma_{21}) + 2(N-2)(N-1)(\sigma_{11}\sigma_{22} - \sigma_{12}\sigma_{21})^2. \quad (20b)$$

Thus, substituting (20) into (12), the explicit expressions of the first two negative moments of  $\xi$  for  $M = 2$  are given as

$$\mathcal{M}_{-1} = -\frac{1}{N-2} + \frac{N\sigma_{11}\sigma_{22}}{(N-2)(\sigma_{11}\sigma_{22} - \sigma_{12}\sigma_{21})} \quad (21)$$

$$\mathcal{M}_{-2} = \frac{\frac{N(N+1)\sigma_{11}^2\sigma_{22}^2}{(\sigma_{11}\sigma_{22} - \sigma_{12}\sigma_{21})^2} - \frac{4N\sigma_{11}\sigma_{22}}{\sigma_{11}\sigma_{22} - \sigma_{12}\sigma_{21}} + 2}{(N-2)(N-3)}. \quad (22)$$

For  $M \geq 3$ , however, it is very difficult to further simplify the expressions in (12) for the first two negative moments of  $\xi$ .

Given the first two negative moments in (12), we are able to approximate the Beta distribution by moment-matching. In particular, for a Beta distribution with density function

$$\frac{1}{B(\alpha, \beta)} z^{\alpha-1} (1-z)^{\beta-1}, \quad z \in [0, 1] \quad (23)$$

where  $B(\alpha, \beta) = \frac{\Gamma(\alpha)\Gamma(\beta)}{\Gamma(\alpha+\beta)}$  is the Beta function, we set its first two negative moments to be equal to the first two negative moments of  $\xi$  given in (12), leading to

$$\mathcal{M}_{-1} = \frac{\alpha + \beta - 1}{\alpha - 1} \quad (24)$$

$$\mathcal{M}_{-2} = \frac{(\alpha + \beta - 1)(\alpha + \beta - 2)}{(\alpha - 1)(\alpha - 2)}. \quad (25)$$

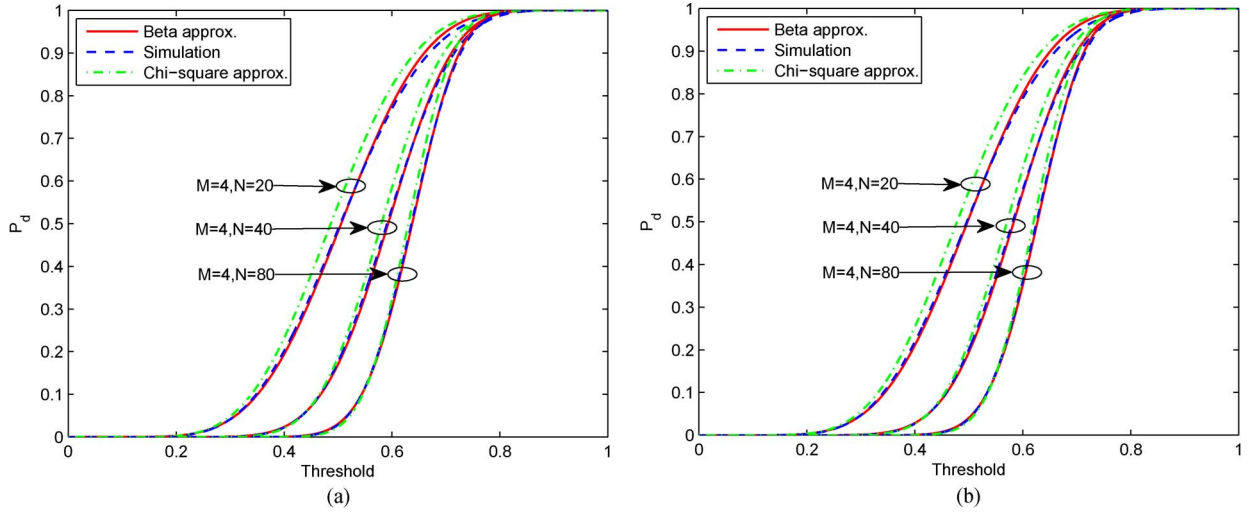


Fig. 1. Detection probability versus threshold for single primary signal in Rayleigh fading channel.  $M = 4$ ,  $\text{SNR} = 2$  dB and  $N = [20, 40, 80]$ . (a) IID noise. (b) Non-IID noises with powers  $[1, 1.7, -0.7, -2]$  dB.

Solving (24) and (25) results in

$$\alpha = \frac{\mathcal{M}_{-1} - \frac{2\mathcal{M}_{-2}}{\mathcal{M}_{-1}} + 1}{\mathcal{M}_{-1} - \frac{\mathcal{M}_{-2}}{\mathcal{M}_{-1}}} \quad (26)$$

$$\beta = (1 - \mathcal{M}_{-1})(1 - \alpha). \quad (27)$$

Recall from (12) that  $\mathcal{M}_{-1} = \mathbb{E}[\xi^{-1}]$  and  $\mathcal{M}_{-2} = \mathbb{E}[\xi^{-2}]$ . As a result, the CDF of  $\xi$  under  $\mathcal{H}_1$  is approximated as

$$F(x) \approx \frac{B_x(\alpha, \beta)}{B(\alpha, \beta)}, \quad x \in [0, 1] \quad (28)$$

where  $B_x(\alpha, \beta) = \int_0^x z^{\alpha-1}(1-z)^{\beta-1}dz$  is the incomplete Beta function.

By matching the moments of  $\xi$  in (12) to those of the Beta distribution, the statistic behavior of  $\xi$  can be approximately determined by the Beta distribution. As the exact moments of  $\xi$  are utilized to calculate  $\alpha$  and  $\beta$  for the Beta distribution in (26) and (27), the CDF of  $\xi$  can be precisely computed by (28). Hence, it follows from (10) that the detection probability is determined as

$$P_d(\gamma) \triangleq \text{Prob}(\xi < \gamma | \mathcal{H}_1) = F(\gamma). \quad (29)$$

Note that the number of partitions of the  $M$ -element set  $\{t_1, \dots, t_M\}$  is the Bell number [38], which significantly increases as  $M$  grows. This thereby indicates that, to accurately determine the theoretical detection probability via (29), the required computational complexity is heavy especially when  $M$  becomes larger. However, as pointed out in [19], the number of antennas in the practical spectrum sensing environments is typically small, say,  $M$  varies from 2 up to 8 due to physical constraints of the device size. Hence, the analytic expression for the detection probability is tractable in the practical spectrum sensing situations. On the contrary, although the exact moments as well as non-null distribution of the Hadamard ratio test for real-valued observation have been studied in [39], their analytic expressions are composed of a sum of infinite terms. Thus, the technique in [39] is intractable for practical sensing applications even though the number of antennas is small.

#### IV. SIMULATION RESULTS

The accuracy of the analytic formula for the detection probability is numerically evaluated in this section. For the purpose of comparison, the empirical detection probability of  $\xi$  and simulation results in [29] by means of asymptotic non-central Chi-square approximation are presented as well. All the numerical results are obtained from  $10^6$  Monte Carlo simulation trials. Fig. 1(a) demonstrates the numerical results for a single primary signal in the Rayleigh fading channel under IID noise, where the number of antennas is 4, the number of samples increases from 20, 40 to 80, and the SNR equals 2 dB. In the Rayleigh fading channel, the entries of  $\mathbf{H} = [\mathbf{h}_1, \dots, \mathbf{h}_d]$  are independently drawn from a standard complex Gaussian distribution, which are fixed during the sensing period but varies in Monte Carlo runs. Without loss of generality, the channel is normalized as  $\mathbf{g}_i = \mathbf{h}_i / \|\mathbf{h}_i\|$ , the noise variance is set to one for IID noise and the averaged noise variance is set to one for non-IID noise. In the sequel, the population covariance matrix is  $\Sigma^{(1)} = \sigma_v \mathbf{I}_M + \sum_{i=1}^d \sigma_{s_i} \mathbf{g}_i \mathbf{g}_i^H$  for IID noise and  $\Sigma^{(1)} = \Sigma^{(0)} + \sum_{i=1}^d \sigma_{s_i} \mathbf{g}_i \mathbf{g}_i^H$  for non-IID noise. Note that  $\sigma_v = \sigma_{v_1} = \dots = \sigma_{v_M}$  for IID noise. It is seen in Fig. 1(a) that the proposed Beta approximation is more accurate than the asymptotic non-central Chi-square approximation in predicting the detection probability. The numerical results for non-IID noise are plotted in Fig. 1(b) in which the powers of the non-IID noises equal  $[1, 1.7, -0.7, -2]$  dB whereas the other parameters remain unchanged. Again, the proposed Beta approximation is superior to the asymptotic non-central Chi-square approximation in terms of accuracy. Similar to [18], [19], to quantitatively demonstrate the accuracy, we employ the Cramér-von Mises criterion [40] to calculate the errors of the non-central Chi-square and proposed Beta approximations with respect to the exact distribution obtained from the simulations. That is,

$$\text{Error} = \frac{1}{10^6} \sum_{i=1}^{10^6} \left| F(x_i) - \hat{F}(x_i) \right|^2 \quad (30)$$

TABLE I  
APPROXIMATION ERROR FOR PROPOSED BETA APPROXIMATION AND ASYMPTOTIC NON-CENTRAL CHI-SQUARE APPROXIMATION WITH RESPECT TO EXACT DISTRIBUTION OF  $\xi$  UNDER  $\mathcal{H}_1$  AT  $M = 4$ ,  $d = 1$  AND SNR = 2 DB IN RAYLEIGH FADING CHANNEL

Method	Proposed Beta Approximation			Asymptotic Chi-square Approximation			
	$N$	20	40	80	20	40	80
Error (IID)		$0.3554 \times 10^{-4}$	$0.1902 \times 10^{-4}$	$0.0937 \times 10^{-4}$	$0.7770 \times 10^{-3}$	$0.4114 \times 10^{-3}$	$0.2237 \times 10^{-3}$
Error (non-IID)		$0.3750 \times 10^{-4}$	$0.1968 \times 10^{-4}$	$0.1084 \times 10^{-4}$	$0.7956 \times 10^{-3}$	$0.4085 \times 10^{-3}$	$0.2070 \times 10^{-3}$

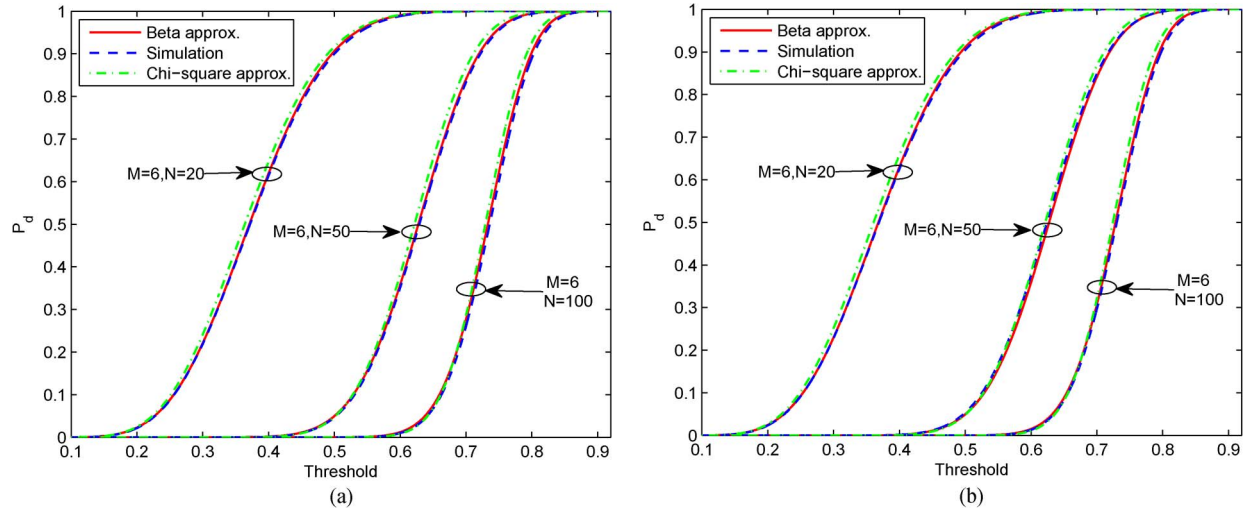


Fig. 2. Detection probability versus threshold for three primary signals in Rayleigh fading channel.  $M = 6$ , SNR =  $[-3, -7, -10]$  dB and  $N = [20, 50, 100]$ . (a) IID noise. (b) Non-IID noises with powers  $[0, -1, 1.5, -0.8, 2, -1.7]$  dB.

TABLE II  
APPROXIMATION ERROR FOR PROPOSED BETA APPROXIMATION AND ASYMPTOTIC NON-CENTRAL CHI-SQUARE APPROXIMATION WITH RESPECT TO EXACT DISTRIBUTION OF  $\xi$  UNDER  $\mathcal{H}_1$  AT  $M = 6$ ,  $d = 3$  AND SNR =  $[-3 - 7 - 10]$  DB IN RAYLEIGH FADING CHANNEL

Method	Proposed Beta Approximation			Asymptotic Chi-square Approximation			
	$N$	20	50	100	20	50	100
Error (IID)		$0.0897 \times 10^{-4}$	$0.1390 \times 10^{-4}$	$0.5892 \times 10^{-4}$	$0.2228 \times 10^{-3}$	$0.2685 \times 10^{-3}$	$0.3291 \times 10^{-3}$
Error (non-IID)		$0.0853 \times 10^{-4}$	$0.4438 \times 10^{-4}$	$0.3051 \times 10^{-4}$	$0.2346 \times 10^{-3}$	$0.0574 \times 10^{-3}$	$0.2684 \times 10^{-3}$

where  $F(x_i)$  is the exact CDF<sup>3</sup> and  $\hat{F}(x_i)$  is its estimate. The error between the approximate and exact distributions of  $\xi$  under the signal-presence hypothesis is tabulated in Table I, where the number of antennas is 4, the number of samples varies from 20, 40 to 80, the number of primary signals is one and the SNR equals 2 dB. It is indicated in Table I that the proposed Beta approximation is much more accurate than its counterpart.

The numerical results for the detection probabilities, proposed Beta approximation and non-central Chi-square approximation versus decision threshold are plotted in Fig. 2, where the number of antennas is 6, the number of samples varies from 20, 50 to 100 and the SNRs for three primary signals equal  $-3$  dB,  $-7$  dB and  $-10$  dB. Fig. 2(a) plots the detection probabilities versus threshold for IID noise. It is observed that the proposed Beta approximation surpasses the asymptotic non-central Chi-square approximation in terms of prediction accuracy. The numerical results for the detection probabilities, proposed Beta approximation and non-central Chi-square approximation in non-IID noise are presented in Fig. 2(b), where the noise variances at the six antennas are set as  $[0, -1,$

$1.5, -0.8, 2, -1.7]$  dB whereas the other parameters remain unchanged. Again, the non-central Chi-square approximation is inferior to the proposed Beta approximation even when the number of samples becomes large, say,  $N = 100$ . Accordingly, Table II presents the errors between the approximate and exact distributions of  $\xi$  under  $\mathcal{H}_1$ . It is observed that the proposed Beta approximation is much more accurate than the non-central Chi-square approximation no matter the noise is IID or non-IID. It is easy to interpret this enhancement in the proposed approximation over the non-central Chi-square approximation because the latter ignores the  $\mathcal{O}(1/N)$  term in the computation of non-centrality parameter. Clearly, this term may be omitted only when  $N$  is sufficiently large. On the contrary, the proposed approach is able to calculate the *exact* first two negative moments, and then utilizes the so-obtained moments to match the parameters of Beta distribution. That is to say, the proposed method does not ignore any terms to determine the approximate Beta distribution.

Now let us evaluate the accuracy of the proposed Beta approximation in terms of receiver operating characteristic (ROC). For comparison, the simulated and Chi-square approximate detection probabilities are provided as well. Moreover, for the purpose of fair comparison, the simulated false-alarm probability is exploited for all the approaches. Fig. 3(a) depicts

<sup>3</sup>Note that the CDF herein corresponds to the detection probability.

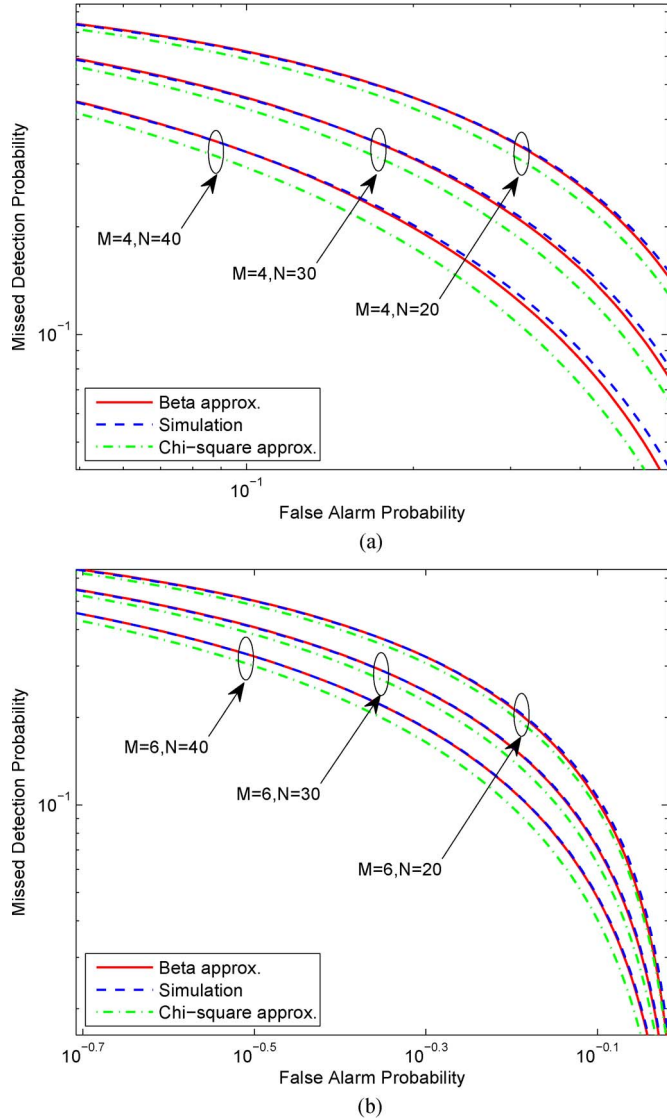


Fig. 3. Missed detection probability versus threshold for IID noise and Rayleigh fading channel with  $N = [20, 30, 40]$ . (a)  $M = 4$ ,  $d = 2$  and  $\text{SNR} = [-3, -5]$  dB. (b)  $M = 6$ ,  $d = 1$  and  $\text{SNR} = -2$  dB.

the numerical results for the scenario of two primary signals and IID noise, where  $M = 4$ ,  $d = 2$ ,  $N = [20, 30, 40]$  and  $\text{SNR} = [-3, -5]$  dB. It is seen that the ROC of the proposed Beta approximation is very close to the exact ROC which is approxi-

mately determined by Monte Carlo simulation. However, since the non-central Chi-square approximation considers  $\mathcal{O}(1/N)$  as sufficiently small and omits it in the calculation of the non-centrality parameter, it cannot provide accurate result particularly for small samples. Fig. 3(b) illustrates the numerical results for another parameter setting in which  $M = 6$ ,  $d = 1$ ,  $\text{SNR} = -2$  dB and  $N = [20, 30, 40]$ . Again, we observe that our proposal is much more accurate than the non-central Chi-square approximation in terms of fitting the exact ROC curves, especially when the number of samples is small.

## V. CONCLUSION

The analytic formula for the detection probability of the Hadamard ratio test has been derived, which provides an efficient approach to theoretically evaluate its sensing performance. By means of calculating the first and second exact negative moments of the test statistic under the signal-presence hypothesis, we are able to approximate the Beta distribution for the signal-presence hypothesis, ending up with accurate analytic expression for the detection probability. Extensive simulation results are in line with our theoretical analysis.

## APPENDIX A PROOF OF PROPOSITION 1

Recall that the SCM  $\mathbf{R}$  under  $\mathcal{H}_1$  follows the complex Wishart distribution  $\mathcal{W}_M(N, \Sigma^{(1)})$  with density function

$$f(\mathbf{R}) \triangleq \frac{1}{\Gamma_M(N) |\Sigma^{(1)}|^N} |\mathbf{R}|^{N-M} \exp\left(\text{tr}[-\Sigma^{(1),-1} \mathbf{R}]\right). \quad (31)$$

The  $k$ -th moment of  $\xi$  can be calculated as (32), shown at the bottom of the page. Here,  $r'_{mm}$  is the  $m$ -th diagonal element of  $\mathbf{R}'$  which is distributed as  $\mathcal{W}_M(N+k, \Sigma^{(1)})$  and  $T = \prod_{i=1}^M r'_{mm}$ . We are now at a position to determine the first two moments of  $T$ .

For  $\mathbf{R}' \sim \mathcal{W}_M(N+k, \Sigma^{(1)})$ , it follows from [41, eq. (5.12)] that the characteristic function is

$$\phi(\Theta) = \left| \mathbf{I}_M - i\Theta \Sigma^{(1)} \right|^{-N-k}. \quad (33)$$

where  $\Theta$  is the matrix argument of the characteristic function. In order to obtain the characteristic function of the diagonal

$$\begin{aligned} \mathbb{E}[\xi^k] &= \int_{\mathbf{R} > 0} \frac{1}{\Gamma_M(N) |\Sigma^{(1)}|^N} |\mathbf{R}|^{N-M} \left( \frac{|\mathbf{R}|}{\prod_{i=1}^M r_{ii}} \right)^k \exp\left(\text{tr}[-\Sigma^{(1),-1} \mathbf{R}]\right) d\mathbf{R} \\ &= \frac{|\Sigma^{(1)}|^k \Gamma_M(N+k)}{\Gamma_M(N)} \int_{\mathbf{R}' > 0} \frac{1}{\Gamma_M(N+k) |\Sigma^{(1)}|^{N+k}} |\mathbf{R}'|^{N-M+k} \left( \prod_{i=1}^M r'_{ii} \right)^{-k} \exp\left(\text{tr}[-\Sigma^{(1),-1} \mathbf{R}']\right) d\mathbf{R}' \\ &= \frac{|\Sigma^{(1)}|^k \Gamma_M(N+k)}{\Gamma_M(N)} \mathbb{E} \left[ \left( \prod_{i=1}^M r'_{ii} \right)^{-k} \right] \triangleq \frac{|\Sigma^{(1)}|^k \Gamma_M(N+k)}{\Gamma_M(N)} \mathbb{E}[T^{-k}] \end{aligned} \quad (32)$$

elements of  $\mathbf{R}'$ , namely,  $r'_{11}, \dots, r'_{MM}$ , we replace  $\Theta$  in (33) with  $\mathbf{D}_t \triangleq \text{diag}(t_1, \dots, t_M)$ , yielding

$$\begin{aligned} & \phi(t_1, \dots, t_M) \\ &= \left| \mathbf{I} - i\mathbf{D}_t \boldsymbol{\Sigma}^{(1)} \right|^{-N-k} \\ &= \begin{vmatrix} 1 - it_1\sigma_{11} & -it_1\sigma_{12} & \cdots & -it_1\sigma_{1M} \\ -it_2\sigma_{21} & 1 - it_2\sigma_{22} & \cdots & -it_2\sigma_{2M} \\ \vdots & \vdots & \ddots & \vdots \\ -it_M\sigma_{M1} & -it_M\sigma_{M2} & \cdots & -it_M\sigma_{MM} \end{vmatrix}^{-N-k} \\ &\triangleq |\mathbf{A}|^{-N-k}. \end{aligned} \quad (34)$$

As a result, the first two moments of  $T$  are calculated as

$$\begin{aligned} T_1 &\triangleq \mathbb{E}[T] = \frac{1}{i^M} \frac{\partial^M \phi(t_1, \dots, t_M)}{\partial t_1 \cdots \partial t_M} \Big|_{\mathbf{D}_t=0} \\ &= \frac{1}{i^M} \frac{\partial^M |\mathbf{A}|^{-N+1}}{\partial t_1 \cdots \partial t_M} \Big|_{\mathbf{D}_t=0} \end{aligned} \quad (35)$$

$$\begin{aligned} T_2 &\triangleq \mathbb{E}[T^2] = \frac{1}{i^{2M}} \frac{\partial^{2M} \phi(t_1, \dots, t_M)}{\partial t_1^2 \cdots \partial t_M^2} \Big|_{\mathbf{D}_t=0} \\ &= \frac{1}{i^{2M}} \frac{\partial^{2M} |\mathbf{A}|^{-N+2}}{\partial t_1^2 \cdots \partial t_M^2} \Big|_{\mathbf{D}_t=0}. \end{aligned} \quad (36)$$

The partial derivatives of  $|\mathbf{A}|^{-N-k}$  with respect to  $t_1, \dots, t_M$  are calculated as follows:

$$\frac{\partial |\mathbf{A}|^{-N-k}}{\partial t_1} = (-1)(N+k) |\mathbf{A}|^{-N-k-1} \frac{\partial |\mathbf{A}|}{\partial t_1} \quad (37)$$

$$\begin{aligned} & \frac{\partial^2 |\mathbf{A}|^{-N-k}}{\partial t_1 \partial t_2} \\ &= (-1)^2 (N+k)(N+k+1) |\mathbf{A}|^{-N-k-2} \frac{\partial |\mathbf{A}|}{\partial t_1} \frac{\partial |\mathbf{A}|}{\partial t_2} \\ &+ (-1)(N+k) |\mathbf{A}|^{-N-k-1} \frac{\partial^2 |\mathbf{A}|}{\partial t_1 \partial t_2} \end{aligned} \quad (38)$$

$$\begin{aligned} & \frac{\partial^3 |\mathbf{A}|^{-N-k}}{\partial t_1 \partial t_2 \partial t_3} \\ &= (-1)^3 (N+k)(N+k+1)(N+k+2) |\mathbf{A}|^{-N-k-3} \\ &\times \frac{\partial |\mathbf{A}|}{\partial t_1} \frac{\partial |\mathbf{A}|}{\partial t_2} \frac{\partial |\mathbf{A}|}{\partial t_3} \\ &+ (-1)^2 (N+k)(N+k+1) |\mathbf{A}|^{-N-k-2} \frac{\partial |\mathbf{A}|}{\partial t_1} \frac{\partial^2 |\mathbf{A}|}{\partial t_2 \partial t_3} \\ &+ (-1)^2 (N+k)(N+k+1) |\mathbf{A}|^{-N-k-2} \frac{\partial^2 |\mathbf{A}|}{\partial t_1 \partial t_2} \frac{\partial |\mathbf{A}|}{\partial t_3} \\ &+ (-1)^2 (N+k)(N+k+1) |\mathbf{A}|^{-N-k-2} \frac{\partial^2 |\mathbf{A}|}{\partial t_1 \partial t_3} \frac{\partial |\mathbf{A}|}{\partial t_2} \\ &+ (-N-k) |\mathbf{A}|^{-N-k-1} \frac{\partial^3 |\mathbf{A}|}{\partial t_1 \partial t_2 \partial t_3} \end{aligned} \quad (39)$$

$$\begin{aligned} & \vdots \\ \frac{\partial^M |\mathbf{A}|^{-N-k}}{\partial t_1 \cdots \partial t_M} &= \sum_{\boldsymbol{\pi} \in \mathcal{S}_M} \frac{\Gamma(N+k+p(\boldsymbol{\pi}))}{\Gamma(N+k)} |\mathbf{A}|^{-N-k-p(\boldsymbol{\pi})} \\ &\times (-1)^{p(\boldsymbol{\pi})} \prod_{m=1}^{p(\boldsymbol{\pi})} \frac{\partial^2 |\mathbf{A}|}{\partial \pi_{m1} \cdots \partial \pi_{mj}}. \end{aligned} \quad (40)$$

Here,  $\mathcal{S}_M$  is composed by all partitions of the  $M$ -element set  $\{t_1, \dots, t_M\}$  with the number of partitions being the Bell number [38],  $\boldsymbol{\pi}$  denotes a partition of  $\{t_1, \dots, t_M\}$  which is defined as a family of nonempty, pairwise disjoint subsets of  $\{t_1, \dots, t_M\}$  whose union is  $\{t_1, \dots, t_M\}$ . Moreover,  $p(\boldsymbol{\pi})$  is the number of subset in  $\boldsymbol{\pi}$ ,  $\pi_m$  is the  $m$ -th subset,  $j$  is the number of elements in  $\pi_m$  and  $\pi_{mj}$  is the  $j$ -th element of  $\pi_m$ .

To illustrate the partitions of  $\{t_1, \dots, t_M\}$  in (40), we take the case of  $M=3$  as an example. The 3-element set  $\{t_1, t_2, t_3\}$  can be partitioned in 5 distinct ways:

$$\begin{aligned} \boldsymbol{\pi} &= \{\{t_1\}, \{t_2\}, \{t_3\}\}, \boldsymbol{\pi}_1 = \{t_1\}, \\ \boldsymbol{\pi}_2 &= \{t_2\}, \boldsymbol{\pi}_3 = \{t_3\}, p(\boldsymbol{\pi}) = 3 \end{aligned} \quad (41a)$$

$$\begin{aligned} \boldsymbol{\pi} &= \{\{t_1\}, \{t_2, t_3\}\}, \boldsymbol{\pi}_1 = \{t_1\}, \\ \boldsymbol{\pi}_2 &= \{t_2, t_3\}, p(\boldsymbol{\pi}) = 2 \end{aligned} \quad (41b)$$

$$\begin{aligned} \boldsymbol{\pi} &= \{\{t_1, t_2\}, \{t_3\}\}, \boldsymbol{\pi}_1 = \{t_1, t_2\}, \\ \boldsymbol{\pi}_2 &= \{t_3\}, p(\boldsymbol{\pi}) = 2 \end{aligned} \quad (41c)$$

$$\begin{aligned} \boldsymbol{\pi} &= \{\{t_1, t_3\}, \{t_2\}\}, \boldsymbol{\pi}_1 = \{t_1, t_3\}, \\ \boldsymbol{\pi}_2 &= \{t_2\}, p(\boldsymbol{\pi}) = 2 \end{aligned} \quad (41d)$$

$$\boldsymbol{\pi} = \{\{t_1, t_2, t_3\}\}, p(\boldsymbol{\pi}) = 1. \quad (41e)$$

Substituting (41) into (40) leads to (39).

As a result, noticing that

$$|\mathbf{A}|_{\mathbf{D}_t=0} = 1 \quad (42)$$

and substituting (40) into (35), we have

$$T_1 = \frac{1}{i^M} \sum_{\boldsymbol{\pi} \in \mathcal{S}_M} \frac{\Gamma(N-1+p(\boldsymbol{\pi}))}{\Gamma(N-1)} (-1)^{p(\boldsymbol{\pi})} \prod_{m=1}^{p(\boldsymbol{\pi})} \nu(\boldsymbol{\pi}_m). \quad (43)$$

Let  $\mathcal{S}_{2M}$  be composed by the partitions of the  $2M$ -element set  $\{t_1, t_1^*, \dots, t_M, t_M^*\}$ , where  $t_m^*$  ( $m=1, \dots, M$ ) is equal to  $t_m$  ( $m=1, \dots, M$ ) in value but different in index. In the sequel, the second-order partial derivative of  $|\mathbf{A}|^{-N-k}$  with respect to  $t_1, \dots, t_M$  amounts to the first-order partial derivative of  $|\mathbf{A}|^{-N-k}$  with respect to  $t_1, t_1^*, \dots, t_M, t_M^*$ . Meanwhile, note that the second- and higher-order partial derivatives of  $|\mathbf{A}|$  with respect to the same variable  $t_m$  are equal to zero. Consequently, substituting (42) along with (40) into (36), we obtain  $T_2$  as

$$T_2 = \frac{1}{i^{2M}} \sum_{\boldsymbol{\pi} \in \mathcal{S}_{2M}} \frac{\Gamma(N-2+p(\boldsymbol{\pi}))}{\Gamma(N-2)} (-1)^{p(\boldsymbol{\pi})} \prod_{m=1}^{p(\boldsymbol{\pi})} \nu(\boldsymbol{\pi}_m). \quad (44)$$

Thus, setting  $k=-1$  and  $k=-2$ , it follows from (32), (43) and (44) that

$$\mathcal{M}_{-1} = \mathbb{E}[\xi^{-1}] = \frac{|\boldsymbol{\Sigma}^{(1)}|^{-1} \Gamma_M(N-1)}{\Gamma_M(N)} T_1 \quad (45)$$

$$\mathcal{M}_{-2} = \mathbb{E}[\xi^{-2}] = \frac{|\boldsymbol{\Sigma}^{(1)}|^{-2} \Gamma_M(N-2)}{\Gamma_M(N)} T_2. \quad (46)$$

This completes the proof of Proposition 1.

## REFERENCES

- [1] "Spectrum-Policy Task Force," Washington, D.C., USA, Rep. ET Docket, 02-135, Nov. 2002.
- [2] J. Mitola, III, "Cognitive radio for flexible mobile multimedia communications," in *Proc. IEEE Int. Workshop MoMuC*, San Diego, CA, USA, Nov. 1999, pp. 3–10.
- [3] S. Haykin, "Cognitive radio: Brain-empowered wireless communications," *IEEE J. Sel. Areas Commun.*, vol. 23, no. 2, pp. 201–220, Feb. 2005.
- [4] R. Zhang and Y. C. Liang, "Exploiting multi-antennas for opportunistic spectrum sharing in cognitive radio networks," *IEEE J. Sel. Topics Signal Process.*, vol. 2, no. 1, pp. 88–102, Feb. 2008.
- [5] Y. Zeng and Y.-C. Liang, "Spectrum-sensing algorithms for cognitive radio based on statistical covariances," *IEEE Trans. Veh. Technol.*, vol. 58, no. 4, pp. 1804–1815, May 2009.
- [6] E. Axell, G. Leus, E. G. Larsson, and H. V. Poor, "Spectrum sensing for cognitive radio: State-of-the-art and recent advances," *IEEE Signal Process. Mag.*, vol. 29, no. 3, May 2012.
- [7] B. Wang and K. J. R. Liu, "Advance in cognitive radio networks: A survey," *IEEE J. Sel. Topics Signal Process.*, vol. 5, no. 1, pp. 5–23, Feb. 2011.
- [8] R. Tandra and A. Sahai, "SNR walls for signal detection," *IEEE J. Sel. Topics Signal Process.*, vol. 2, no. 1, pp. 4–17, Feb. 2008.
- [9] H. Urkowitz, "Energy detection of unknown deterministic signals," *Proc. IEEE*, vol. 55, no. 4, pp. 523–531, Apr. 1967.
- [10] F. F. Digham, M. S. Alouini, and M. K. Simon, "On the energy detection of unknown signals over fading channels," *IEEE Trans. Commun.*, vol. 55, no. 1, pp. 21–24, Jan. 2007.
- [11] A. Mariani, A. Giorgetti, and M. Chiani, "Effects of noise power estimation on energy detection for cognitive radio applications," *IEEE Trans. Commun.*, vol. 59, no. 12, pp. 3410–3420, Dec. 2011.
- [12] Y. Zeng, C. L. Koh, and Y.-C. Liang, "Maximum eigenvalue detection: Theory and application," in *Proc. IEEE ICC*, Beijing, China, May 2008, pp. 4160–4164.
- [13] T. J. Lim, R. Zhang, Y. C. Liang, and Y. H. Zeng, "GLRT-based spectrum sensing for cognitive radio," in *Proc. IEEE GLOBECOM*, New Orleans, LA, USA, Dec. 2008, pp. 1–5.
- [14] Y. Zeng and Y.-C. Liang, "Eigenvalue-based spectrum sensing algorithms for cognitive radio," *IEEE Trans. Commun.*, vol. 57, no. 6, pp. 1784–1793, Jun. 2009.
- [15] B. F. Penna, R. Garello, and M. A. Spirito, "Cooperative spectrum sensing based on the limiting eigenvalue ratio distribution in Wishart matrices," *IEEE Commun. Lett.*, vol. 13, no. 7, pp. 507–509, Jul. 2009.
- [16] A. Kortun, T. Ratnarajah, M. Sellathurai, C. Zhong, and C. B. Papadias, "On the performance of eigenvalue-based cooperative spectrum sensing for cognitive radio," *IEEE J. Sel. Topics Signal Process.*, vol. 5, no. 1, pp. 49–55, Feb. 2011.
- [17] P. Wang, J. Fang, N. Han, and H. Li, "Multiantenna-assisted spectrum sensing for cognitive radio," *IEEE Trans. Veh. Technol.*, vol. 59, no. 4, pp. 1791–1800, May 2010.
- [18] L. Wei, P. Dharmawansa, and O. Tirkkonen, "Multiple primary user spectrum sensing in the low SNR regime," *IEEE Trans. Commun.*, vol. 61, no. 5, pp. 1720–1731, May 2013.
- [19] L. Wei and O. Tirkkonen, "Spectrum sensing in the presence of multiple primary users," *IEEE Trans. Commun.*, vol. 60, no. 5, pp. 1268–1277, May 2012.
- [20] S. Wilks, "On the independence of  $k$  sets of normally distributed statistical variables," *Econometrica*, vol. 3, no. 3, pp. 309–326, Jul. 1935.
- [21] A. Leshem and A.-J. van der Veen, "Multichannel detection of Gaussian signals with uncalibrated receivers," *IEEE Signal Process. Lett.*, vol. 8, no. 4, pp. 120–122, Apr. 2001.
- [22] A. Leshem and A.-J. van der Veen, "Multichannel detection and spatial signature estimation with uncalibrated receivers," in *Proc. 11th IEEE Workshop Stat. Signal Process.*, Singapore, Dec. 2001, pp. 190–193.
- [23] R. Li, L. Huang, Y. Shi, and H. C. So, "Gerschgorin disk-based robust spectrum sensing for cognitive radio," in *Proc. IEEE ICASSP*, Florence, Italy, May 2014, pp. 1–4.
- [24] J. Vía, D. Ramírez, and I. Santamaría, "The locally most powerful test for multiantenna spectrum sensing with uncalibrated receivers," in *Proc. IEEE ICASSP*, Kyoto, Japan, Mar. 2012, pp. 3437–3440.
- [25] D. Ramírez, J. Vía, I. Santamaría, and L. L. Scharf, "Locally most powerful invariant tests for correlation and sphericity of Gaussian vectors," *IEEE Trans. Inf. Theory*, vol. 59, no. 4, pp. 2128–2141, Apr. 2013.
- [26] L. Huang, H. C. So, and C. Qiang, "Volume-based method for spectrum sensing," *Dig. Signal Process.*, vol. 28, pp. 48–56, May 2014.
- [27] D. Ramírez, G. Vazquez-Vilar, R. López-Valcarce, J. Vía, and I. Santamaría, "Detection of rank- $p$  signals in cognitive radio networks with uncalibrated multiple antennas," *IEEE Trans. Signal Process.*, vol. 59, no. 8, pp. 3764–3774, Aug. 2011.
- [28] R. López-Valcarce, G. Vazquez-Vilar, and J. Sala, "Multiantenna spectrum sensing for cognitive radio: Overcoming noise uncertainty," in *Proc. IEEE Int. Workshop CIP*, Elba Island, Italy, Jun. 2010, pp. 310–315.
- [29] J. K. Tugnait, "On multiple antenna spectrum sensing under noise variance uncertainty and flat fading," *IEEE Trans. Signal Process.*, vol. 60, no. 4, pp. 1823–1832, Apr. 2012.
- [30] A. Mariani, A. Giorgetti, and M. Chiani, "Test of independence for cooperative spectrum sensing with uncalibrated receivers," in *Proc. IEEE GLOBECOM*, Anaheim, CA, USA, Dec. 2012, pp. 1374–1379.
- [31] A. Taherpour, M. Nasiri-Kenari, and S. Gazor, "Multiple antenna spectrum sensing in cognitive radios," *IEEE Trans. Wireless Commun.*, vol. 9, no. 2, pp. 814–823, Nov. 2010.
- [32] J. D. Williams, "Moments of the ratio of the mean square successive difference to the mean square difference in samples from a normal universe," *Ann. Math. Statist.*, vol. 12, no. 2, pp. 239–241, 1941.
- [33] N. Cressie, A. S. Davis, J. L. Folks, and G. E. Policello, II, "The moment-generating function and negative integer moments," *Amer. Statistician*, vol. 35, no. 3, pp. 148–150, Aug. 1981.
- [34] Y. V. Fyodorov, "Negative moments of characteristic polynomials of random matrices: Ingham–Siegel integral as an alternative to Hubbard–Stratonovich transformation," *Nucl. Phys. B*, vol. 621, no. 3, pp. 643–674, Jan. 2002.
- [35] R. A. Horn and C. R. Johnson, *Matrix Analysis*. Cambridge, U.K.: Cambridge Univ. Press, 1985.
- [36] S. John, "Fitting sampling distribution agreeing in support and moments and tables of critical values of sphericity criterion," *J. Multivariate Anal.*, vol. 6, no. 4, pp. 601–607, Dec. 1976.
- [37] A. Giorgetti and M. Chiani, "A new approach to time-of-arrival estimation based on information theoretic criteria," in *Proc. IEEE ICUBW*, Bologna, Italy, Sep. 2011, pp. 460–464.
- [38] G. Rota, "The number of partitions of a set," *Amer. Math.*, vol. 71, no. 5, pp. 498–504, May 1964.
- [39] A. M. Mathai and W. Y. Tan, "The non-null distribution of the likelihood ratio criterion for testing the hypothesis that the covariance matrix is diagonal," *Can. J. Statist.*, vol. 5, no. 1, pp. 63–74, 1977.
- [40] T. W. Anderson, "On the distribution of the two-sample Cramér–Von Mises criterion," *Ann. Math. Statist.*, vol. 33, no. 3, pp. 1148–1159, Sep. 1962.
- [41] N. R. Goodman, "Statistical analysis based on a certain multivariate complex Gaussian distribution (an introduction)," *Ann. Math. Stat.*, vol. 34, no. 1, pp. 152–177, Mar. 1963.



**Lei Huang** (M'07) was born in Guangdong, China. He received the B.Sc., M.Sc., and Ph.D. degrees from Xidian University, Xi'an, China, in 2000, 2003, and 2005, respectively, all in electronic engineering.

From 2005 to 2006, he was a Research Associate with the Department of Electrical and Computer Engineering, Duke University, Durham, NC, USA. From 2009 to 2010, he was a Research Fellow with the Department of Electronic Engineering, City University of Hong Kong, Kowloon, Hong Kong, and a Research Associate with the Department of

Electronic Engineering, The Chinese University of Hong Kong, Shatin, Hong Kong. Since 2011, he has been with the Department of Electronic and Information Engineering, Harbin Institute of Technology Shenzhen Graduate School, Shenzhen, China, where he is currently a Professor. His research interests include spectral estimation, array signal processing, statistical signal processing, and their applications in radar and wireless communication systems.

Dr. Huang is currently an Editorial Board Member of *Digital Signal Processing*.



**Yuhang Xiao** was born in Anhui, China, on January 20, 1992. He received the B.E. degree from Harbin Engineering University, Harbin, China, in 2012. He is currently working toward the Ph.D degree in communication and information engineering with Harbin Institute of Technology Shenzhen Graduate School, Shenzhen, China. His research interests include statistical signal processing and spectrum sensing.



**Hing Cheung So** (S'90–M'95–SM'07) was born in Hong Kong. He received the B.Eng. degree in electronic engineering from the City University of Hong Kong, Kowloon, Hong Kong, in 1990 and the Ph.D. degree in electronic engineering from The Chinese University of Hong Kong, Shatin, Hong Kong, in 1995. From 1990 to 1991, he was an Electronic Engineer with the Research and Development Division, Everex Systems Engineering Ltd., Hong Kong. During 1995–1996, he was a Postdoctoral Fellow with The Chinese University of

Hong Kong. From 1996 to 1999, he was a Research Assistant Professor with the Department of Electronic Engineering, City University of Hong Kong, where he is currently an Associate Professor. His research interests include statistical signal processing, fast and adaptive algorithms, signal detection, parameter estimation, and source localization.

Dr. So was an Associate Editor of the *IEEE TRANSACTIONS ON SIGNAL PROCESSING* during 2010–2014. Currently, he is on the Editorial Board of *IEEE Signal Processing Magazine*, *Signal Processing*, and *Digital Signal Processing*, as well as a member of the Signal Processing Theory and Methods Technical Committee of the IEEE Signal Processing Society.



**Jun Fang** (M'08) received the B.S. and M.S. degrees from Xidian University, Xi'an, China, in 1998 and 2001, respectively, and the Ph.D. degree from the National University of Singapore, Singapore, in 2006, all in electrical engineering.

In 2006, he was a Postdoctoral Research Associate with the Department of Electrical and Computer Engineering, Duke University, Durham, NC, USA. From January 2007 to December 2010, he was a Research Associate with the Department of Electrical and Computer Engineering, Stevens Institute of Technology, Hoboken, NJ, USA. Since January 2011, he has been with the University of Electronic Science and Technology of China, Chengdu, China. His current research interests include statistical signal processing, sparse theory and compressed sensing, and Bayesian statistical inference.

Dr. Fang received the IEEE Vehicular Technology Society Jack Neubauer Memorial Award in 2013 and the IEEE Africon Outstanding Paper Award in 2011. He is an Associate Technical Editor of the *IEEE Communications Magazine* and an Associate Editor of the *IEEE SIGNAL PROCESSING LETTERS*.